

Cloud effects on the surface energy and mass balance of Brewster Glacier

J. P. Conway and
N. J. Cullen

Cloud effects on the surface energy and mass balance of Brewster Glacier, New Zealand

J. P. Conway^{1,2} and N. J. Cullen¹

¹Department of Geography, University of Otago, Dunedin, New Zealand

²Centre for Hydrology, University of Saskatchewan, Saskatoon, Canada

Received: 19 January 2015 – Accepted: 31 January 2015 – Published: 18 February 2015

Correspondence to: J. P. Conway (jonathan.conway@usask.ca)

Published by Copernicus Publications on behalf of the European Geosciences Union.

Title Page

Abstract

Introduction

Conclusions

References

Tables

Figures

◀

▶

◀

▶

Back

Close

Full Screen / Esc

Printer-friendly Version

Interactive Discussion

Abstract

A thorough understanding of the influence of clouds on glacier surface energy balance (SEB) and surface mass balance (SMB) is critical for forward and backward modelling of glacier–climate interactions. A validated 22 month time series of SEB/SMB was constructed for the ablation zone of the Brewster Glacier, using high quality radiation data to carefully evaluate SEB terms and define clear-sky and overcast conditions. A fundamental change in glacier SEB in cloudy conditions was driven by increased effective sky emissivity and surface vapour pressure, rather than the minimal change in air temperature and wind speed. During overcast conditions, positive net longwave radiation and latent heat fluxes allowed melt to be maintained through a much greater length of time compared to clear-sky conditions, and led to similar melt in each sky condition. The sensitivity of SMB to changes in air temperature was greatly enhanced in overcast compared to clear-sky conditions due to more frequent melt and the occurrence of precipitation, which enabled a strong accumulation–albedo feedback. During the spring and autumn seasons, the sensitivity during overcast conditions was strongest. There is a need to include the effects of atmospheric moisture (vapour, cloud and precipitation) on melt processes when modelling glacier–climate interactions.

1 Introduction

The response of glaciers to atmospheric forcing is of interest as glaciers are seen as useful scalable proxy records of past climate (e.g. Mölg et al., 2009a) and because the rapid changes occurring in many glaciated regions have implications for both global sea level rise (Kaser et al., 2006) and water resources (e.g. Jost et al., 2012). Reliable attribution of past glacier states and prediction of future ones is dependent on a thorough understanding of the physical processes operating at the glacier surface that link glacier change with climate, that is, the surface mass balance (SMB) and surface energy balance (SEB). For debris free, mid-latitude glaciers, the SMB is primarily a prod-

TCD

9, 975–1019, 2015

Cloud effects on the surface energy and mass balance of Brewster Glacier

J. P. Conway and
N. J. Cullen

Title Page

Abstract

Introduction

Conclusions

References

Tables

Figures

◀

▶

◀

▶

Back

Close

Full Screen / Esc

Printer-friendly Version

Interactive Discussion



Cloud effects on the surface energy and mass balance of Brewster Glacier

J. P. Conway and
N. J. Cullen

Title Page

Abstract

Introduction

Conclusions

References

Tables

Figures

◀

▶

◀

▶

Back

Close

Full Screen / Esc

Printer-friendly Version

Interactive Discussion

uct of the relative magnitudes of accumulated solid precipitation and melt. While, in general, incoming shortwave radiation (SW↓) is the major source of energy for glacier melt, variations in SMB are considered to be forced by changes in air temperature and precipitation (Oerlemans, 2005) through both accumulation and melt processes.

A strong positive feedback between accumulation and surface albedo accounts for much of the sensitivity to both air temperature and precipitation, along with the often efficient relationship between air temperature and melt. The mechanisms responsible for the temperature dependence of melt vary widely (Sicart et al., 2008), and include the variability of turbulent sensible (QS) and latent (QL) heat fluxes, incoming longwave radiation (LW↓), and a (somewhat spurious) covariance between air temperature and SW↓ in many continental areas. The primary influence of air temperature on melt rate is also nuanced by other influences on the SEB such as surface albedo (Oerlemans et al., 2009), humidity (Gillett and Cullen, 2011), and cloud transmission (Pellicciotti et al., 2005).

The influence of clouds on the SEB is, in fact, far more pervasive. Recent advances in AWS deployment on glacier surfaces (Mölg et al., 2009b), the availability of high-quality radiation measurements (van den Broeke et al., 2004), and development of methods to extract information about cloud cover in data sparse areas (Kuipers Munneke et al., 2011), have allowed the variation of SEB and SMB with cloud cover to be characterised in many areas. Sicart et al. (2010) show clouds dominate day to day variations in LW↓ in mountainous areas while numerous studies detail the fundamental changes in SEB with cloudiness that are often co-incident with changes in glacier surface boundary layer (SBL) properties (van den Broeke et al., 2006; Giesen et al., 2008; Gillett and Cullen, 2011). Given their strong control on the SEB, and coincidence with changes in SBL properties it is vital that the role of clouds in altering the sensitivity of SMB to changes in atmospheric state variables (especially air temperature) be assessed.

The glaciers of the Southern Alps of New Zealand occupy a unique position in the westerly wind belt of the Southern Ocean, a region dominated by mid-latitude atmospheric circulation (Tait and Fitzharris, 1998; Ummenhofer and England, 2007). The

Cloud effects on the surface energy and mass balance of Brewster Glacier

J. P. Conway and
N. J. Cullen

Title Page

Abstract

Introduction

Conclusions

References

Tables

Figures

◀

▶

◀

▶

Back

Close

Full Screen / Esc

Printer-friendly Version

Interactive Discussion

large barrier the Southern Alps poses to the prevailing winds creates a high precipitation environment, which, coupled to the relatively low elevation of glacier termini (Hoelzle et al., 2007), creates high mass turnover glaciers that have shown high sensitivity to climatic variations in temperature-index glacier modelling studies (Anderson et al., 2006; Oerlemans, 2010). For these reasons the glaciers of the Southern Alps are seen as useful indicators of regional atmospheric circulation in the southwest Pacific and form a vital component of paleoclimate work (e.g. Lorrey et al., 2007). While accumulation–albedo feedbacks have been shown to be important to the sensitivity of SMB to air temperature in New Zealand as in other glaciated regions (Oerlemans, 1997; Anderson et al., 2006), there is a suggestion that increased turbulent (mainly sensible) heat fluxes dominate variations in melt (Anderson et al., 2010). This has led some authors to interpret past glacier fluctuations as a linear and direct proxy for regional air temperature (e.g. Putnam et al., 2012), at the exclusion of most other elements of the glacier–climate system.

It has been well established that synoptic scale processes exert a strong control on the SMB in the Southern Alps, with periods of 20th Century glacier advance and retreat associated with anomalies in the regional climate system (Fitzharris et al., 2007). Given that this synoptic variability is closely linked to inferred changes in cloudiness as well as air mass properties (Hay and Fitzharris, 1988), and that these synoptic controls are thought to have varied over paleo-climatic timescales (Drost et al., 2007; Ackerley et al., 2011), it is vital that the influence of clouds on SMB is separated out from the influence of air mass properties (in particular air temperature). Recent field studies on the Brewster Glacier, Southern Alps, have shown the high frequency of cloudy conditions during all seasons (> 50 % overcast conditions) as well as the significant and variable effect of clouds on $SW\downarrow$, $LW\downarrow$ and net radiation (Rnet) (Conway et al., 2014). In this context it is timely to examine in detail the influence of clouds on glacier surface climate, SEB and melt, as well as the manner in which clouds alter the sensitivity of SMB to air temperature in the Southern Alps.

Cloud effects on the surface energy and mass balance of Brewster Glacier

J. P. Conway and
N. J. Cullen

Title Page

Abstract

Introduction

Conclusions

References

Tables

Figures

◀

▶

◀

▶

Back

Close

Full Screen / Esc

Printer-friendly Version

Interactive Discussion

This paper addresses these issues by resolving the SEB and SMB at a site in the ablation zone of the Brewster Glacier over a 22 month period. High quality surface climate data presented in Cullen and Conway (2015) are used to force a SMB model (Mölg et al., 2008) to estimate both SEB and SMB terms over this period (measurement period). The cloud metrics presented in Conway et al. (2014) are used to identify clear-sky and overcast conditions and thus characterise surface climate, SEB and melt energy during each condition. To test the sensitivity of SMB to changes in surface climate and radiative components, a more heavily parameterised version of the model is run over a hybrid two-year dataset (sensitivity period), allowing the effect of changes in surface climate and radiative properties to be assessed independently and the influence of clouds on this sensitivity to be assessed. The following section provides a brief description of the site, datasets and modelling methods before the results and discussion are presented in subsequent sections.

2 Methods

2.1 Site description and instrumentation

The Brewster Glacier is a small mountain glacier situated in the Southern Alps immediately west of the main divide (Fig. 1). It experiences a temperate maritime high precipitation environment, with annual precipitation around 6000 mm water equivalent (w.e.) and an annual temperature of 1.2 °C over the glacier surface at 1760 m a.s.l. (Cullen and Conway, 2015). In comparison to other glaciers in the Southern Alps, it has a somewhat lower average slope (16°) but similar mean elevation and elevation of the glacier snout (Hoelzle et al., 2007). As it is located on the main divide with relatively high exposure to synoptic weather systems, at the midpoint of the north–south distribution of glaciers in the Southern Alps (Chinn et al., 2012), it is likely to experience the atmospheric controls on SMB that affect the Southern Alps in general.

Cloud effects on the surface energy and mass balance of Brewster Glacier

J. P. Conway and
N. J. Cullen

Title Page

Abstract

Introduction

Conclusions

References

Tables

Figures

◀

▶

◀

▶

Back

Close

Full Screen / Esc

Printer-friendly Version

Interactive Discussion



Data from an automatic weather station (AWS) situated in the ablation area of Brewster Glacier (AWS_{glacier}) were used in this study (Fig. 1). Table 1 gives details of instrumentation and annual average surface climate variables at AWS_{glacier}, while further details of the locality and AWS instrumentation can be found in Cullen and Conway (2015). Measurements at AWS_{glacier} ran for 22 months from 25 October 2010 to 1 September 2012 (inclusive). Air temperature (T_a) shows a moderate seasonal cycle (8 °C), and airmass changes appear to override the subdued diurnal range in T_a . Wind speed (U) is moderate with a persistent down-glacier flow despite the small fetch and exposed location (Conway, 2013). Humidity is high with average vapour pressure exceeding that of a melting surface through 4 months during summer. Cloud cover is frequent and associated with on-glacier wind direction (Conway et al., 2014). Annual mass balance in the vicinity of AWS_{glacier} is generally negative, despite the large accumulation (> 3 m w.e.) of winter snowfall during May through September. The significant annual ablation (> 4 m w.e.) generally starts during October, exposing an ice surface in early January and continuing till April or later.

2.2 Data treatment and cloud metrics

Cullen and Conway (2015) describe the treatment of the AWS data in detail but a summary of the main steps is given here. T_a data were corrected for the (large) influence of solar radiation on the un aspirated shields, resulting in a 0.7 °C decrease in mean annual T_a . To facilitate SMB modelling, a continuous precipitation dataset (P_{scaled}) was constructed by comparing summer rain gauge observations from a second AWS situated in the pro-glacial area (AWS_{lake}) to a nearby lowland rain gauge ($R^2 = 0.9$ at daily level).

To construct a high temporal resolution record of observed SMB, surface height observed using a sonic ranger (Cullen and Conway, 2015) was combined with periodic snow density measurements. Snow pits near the start of snowmelt indicated a consistent density approaching 500 kg m⁻³ during late October (443 kg m⁻³ on 23 October 2010; 483 kg m⁻³ on 27 October 2011), while density during mid-winter was more

Cloud effects on the surface energy and mass balance of Brewster Glacier

J. P. Conway and
N. J. Cullen

Title Page

Abstract

Introduction

Conclusions

References

Tables

Figures

◀

▶

◀

▶

Back

Close

Full Screen / Esc

Printer-friendly Version

Interactive Discussion



moderate (320 kg m^{-3} on 18 July 2011). Thus, while the density of melting snow during spring is relatively well constrained, the increasing density due to subsurface processes (e.g. viscous compaction and melt–refreezing) during the winter months produces some uncertainty in the relationship between surface height and SMB. Beyond the snow-ice transition in early January, a standard ice density of 900 kg m^{-3} was assumed, while short periods of new snowfall were assigned a fresh snow density of 300 kg m^{-3} (Gillett and Cullen, 2011).

A record of cloudiness was constructed using measurements of $\text{LW}\downarrow$ and a clear-sky emissivity model (Conway et al., 2014). The longwave equivalent cloudiness (N_ε) scales the effective sky emissivity (from observed $\text{LW}\downarrow$) between the modelled clear-sky emissivity and an overcast emissivity of 1. Though not directly comparable to traditional cloud fraction metrics based on manual or sky camera observations, N_ε very effectively characterises the effects of clouds on surface radiation fluxes. It also has the advantage over metrics based on $\text{SW}\downarrow$, in that it provides 24 h coverage and is not affected by solar zenith angle or multiple reflections between the surface and atmosphere.

2.3 Model description

A SMB model (Mölg et al., 2008) was used to resolve surface energy and mass fluxes at $\text{AWS}_{\text{glacier}}$ for the full 22 month study period. A full description of the model is given in Mölg et al. (2008, 2009a), but a short description of the parameterisation of each term is given here. The model computes SMB as the sum of snow accumulation, melt, refreezing of liquid water in the snowpack and mass fluxes of water vapour (deposition and sublimation) while surface temperature (T_s) is less than 0°C . Fluxes of vapour while the surface temperature is melting are not included directly in the SMB, as condensation and evaporation are assumed to add and remove mass from the liquid melt water at the surface, respectively. The model uses T_s as a free variable to close the SEB (Eq. 1) at each 30 min timestep:

$$\text{QM} = \text{SW}\downarrow (1 - \alpha) + \text{LW}\downarrow - \sigma \varepsilon T_s^4 + \text{QS} + \text{QL} + \text{QR} + \text{QC} \quad (1)$$

Cloud effects on the surface energy and mass balance of Brewster Glacier

J. P. Conway and
N. J. Cullen

Title Page

Abstract

Introduction

Conclusions

References

Tables

Figures

◀

▶

◀

▶

Back

Close

Full Screen / Esc

Printer-friendly Version

Interactive Discussion

where QM is the energy for surface melt while $T_s = 0^\circ\text{C}$, $\text{SW}\downarrow$ is the incoming solar radiation, α is the albedo, $\text{LW}\downarrow$ is the incoming longwave radiation, σ is the Stefan–Boltzman constant ($5.67 \times 10^{-8} \text{ W m}^{-2}$), ε is the emissivity of snow/ice (equal to unity), T_s is the surface temperature (K), QS and QL are the turbulent sensible and latent heat fluxes, respectively, QR is the rain heat flux and QC is the conductive heat flux through the glacier subsurface. The convention used is that energy fluxes directed towards the surface are positive.

Two different configurations of the model are presented in this paper, distinguished only by their treatment of surface radiation fluxes. For the first, SEBmr, we used measured values of $\text{SW}\downarrow$, $\text{LW}\downarrow$ and α from $\text{AWS}_{\text{glacier}}$ (Table 2) to provide best estimates of SEB and SMB terms for analysis. For the second, SEBpr, we used parameterised radiation fluxes (Table 2) to assess the sensitivity of the SMB to changes in surface climate (detailed further in Sect. 2.5). All other energy fluxes are calculated consistently between configurations. QR is calculated using P_{scaled} assuming rain temperature is equal to T_a . New snow was calculated from P_{scaled} using a rain/snow threshold ($T_{r/s}$) of 1°C and a fixed density of 300 kg m^{-3} . The iterative SEB closure scheme of Mölg et al. (2008) was used to calculate T_s , with QC being calculated as the flux between the surface and the top layer of the twelve layer subsurface module (subsurface levels: 0.1, 0.2, 0.3, 0.4, 0.5, 0.8, 1.4, 2, 3, 5, and 7 m). Penetrating shortwave radiation was not included in the model, as the sub surface temperature profile was not measured throughout the study period; hence the optimisation of a penetrating shortwave radiation scheme would be subject to large uncertainty. The depth, density and temperature (iso-thermal at 0°C) of the snowpack was prescribed at the start of the measurement period from snow-pit measurements (see Sect. 2.2).

The turbulent heat fluxes, QS and QL, were calculated using a bulk-aerodynamic approach using the C_{\log} parameterisation as described by Conway and Cullen (2013). The roughness lengths for momentum (z_{0v}), temperature (z_{0t}) and humidity (z_{0q}) over an ice surface at $\text{AWS}_{\text{glacier}}$ are well constrained by in-situ measurements ($z_{0v} = 3.6 \times 10^{-3} \text{ m}$, $z_{0t} = z_{0q} = 5.5 \times 10^{-5} \text{ m}$; Conway and Cullen, 2013), though spatial and

Cloud effects on the surface energy and mass balance of Brewster Glacier

J. P. Conway and
N. J. Cullen

Title Page

Abstract

Introduction

Conclusions

References

Tables

Figures

◀

▶

◀

▶

Back

Close

Full Screen / Esc

Printer-friendly Version

Interactive Discussion

temporal variability is still probable. A further period of eddy covariance measurements over a spring snow surface (27 October to 3 November 2011) showed a log-mean value for z_{0v} of 1.8×10^{-3} m ($\sigma = 1.3 \times 10^{-2}$ m, $n = 31$), using the same filtering criterion as Conway and Cullen (2013). No reliable estimates of z_{0t} or z_{0q} were possible because of the large uncertainties involved with the small temperature and vapour pressure gradients experienced during this period. Given the similar, but more uncertain, z_{0v} over snow and the large effect of z_{0t} on the effective roughness length which tends to counter a change in z_{0v} (Conway and Cullen, 2013), roughness lengths derived over ice were adopted for the entire period.

2.4 Estimation of uncertainty using a Monte Carlo approach

To estimate uncertainty in modelled SMB, a series of Monte Carlo simulations were made covering the range of input data and parameter uncertainty expected for each configuration of the model (SEBmr and SEBpr). Table 3 shows the parameter uncertainty introduced for each configuration, while input data uncertainty was kept consistent with that used in Conway and Cullen (2013) and is given in Table 1. For both configuration, 5000 runs of the measurement period were made, with systematic and random errors being assigned to each input variable before each simulation and time step, respectively. Errors were calculated by multiplying the uncertainties associated with each input variable (Tables 1 and 3) by normally distributed random numbers ($\mu = 0$; $\sigma = 1$), with the exception of z_{0v} which was logarithmically transformed before the uncertainty was applied. The 5000 SMB time series computed for each configuration were subjected to a first order check, using measured T_s as a proxy for a realistic evaluation of the SEB. Runs were removed when 30 min modelled T_s had root mean squared differences (RMSD) > 1.5 K or $R^2 < 0.9$, which removed $\sim 10\%$ of runs from each ensemble. The remaining runs were then used to compute an ensemble mean and SD for the SMB accumulated over one-day and 10 day periods in addition to the full measurement period. Runs that did not correctly predict the accumulated SMB at the end of the measurement period were not removed, as it was unknown if any systematic

Cloud effects on the surface energy and mass balance of Brewster Glacier

J. P. Conway and
N. J. Cullen

Title Page

Abstract

Introduction

Conclusions

References

Tables

Figures

◀

▶

◀

▶

Back

Close

Full Screen / Esc

Printer-friendly Version

Interactive Discussion

of the underlying surface. Secondly, a daily total snowfall in excess of 5 cm (depth) was introduced as a threshold above which the new snowfall impacts albedo, as small snowfalls are likely to be redistributed into crevasses and hollows on the glacier surface and have minimal impact on the albedo. These two modifications removed large positive feedbacks in the scheme that often caused small snowfalls to increase albedo long after the model had removed the new snow by melting.

An analysis of measured albedo (α_{acc}) at $AWS_{glacier}$ allowed local values of α_{frsnow} (0.95), α_{firn} (0.65) and α_{ice} (0.42) to be defined (Fig. 2a). The higher local values are likely indicative of lower levels of contaminants that are responsible for decreased albedo (Oerlemans et al., 2009) and a lack of debris surrounding the Brewster Glacier. A better fit to the evolution of measured albedo was found by decreasing t^* to 10 days, which seems reasonable given the higher rate of melt (and therefore snow metamorphism) in this maritime environment. Figure 2a also shows a marked difference between the ice surface albedo between the two seasons. It is unclear if this difference reflects changes over a large spatial scale or if a localised increase in sediment observed in the vicinity of $AWS_{glacier}$ during the summer of 2012 contributed to the decrease in albedo during the second season. Without a clear basis for this variation, a mean value of $\alpha_{ice} = 0.42$ is adopted for both seasons.

ΔSMB was computed by conducting runs with SEBpr over the sensitivity period, introducing a range of systematic perturbations to input data and parameters (introduced with the results in Table 6) and comparing SMB between each run. To calculate variations in ΔSMB with cloudiness, ΔSMB was computed at each model timestep (i.e. $\text{mm w.e. } 30 \text{ min}^{-1}$) for each perturbation run. Model timesteps were then selected based on cloudiness (N_{ϵ}) and a monthly average produced for clear-sky and overcast conditions. For ease of interpretation, ΔSMB was converted to a daily rate (mm w.e. day^{-1}) by multiplying by the number of model timesteps within a day (48). By definition, the sum of ΔSMB for each timestep within a year is equal to the accumulated ΔSMB of the entire year, which is the more commonly reported value (e.g. $1.5 \text{ mm w.e. a}^{-1}$).

3 Results

3.1 Model evaluation

Both configurations of the SMB model (SEBmr and SEBpr) were first validated against observed T_s and SMB during the measurement period. Modelled T_s from reference runs of both configurations agreed well with T_s calculated from measurements of outgoing longwave radiation (Fig. 3). Both mean bias error (MBE) and RMSD at 30 min timesteps were comparable to similar studies (van den Broeke et al., 2011), and monthly averages indicated no seasonally dependant errors in the SEB. Figure 2b shows the large accumulation and ablation experienced at AWS_{glacier} during the measurement period. Winter accumulations were fairly consistent between 1.5 and 1.8 m w.e., while summer ablation was more variable. In general, both configurations of the model gave fairly close agreement to the observed accumulated SMB over the measurement period. Both gave SMB during the first accumulation season within $\pm 10\%$ of that observed (Table 4), which was encouraging given the uncertainties in the scaled precipitation dataset and rain/snow threshold. SEBmr showed small discrepancies in modelled ablation (around 10%) for the ice surface in the first season and the snow surface in the second season (Table 4). SEBpr showed similar performance, with an underestimate of ablation for ice surface in the second season likely related to the lower measured α in this season (Fig. 2a). Despite these small deviations, both configurations produced SMB over the two seasons that was well within the accumulated uncertainty due to measurement and parameter errors (grey shading in Fig. 2b). The small discrepancies between modelled and observed ablation could have been removed, perhaps through specifying different z_{ov} for snow and ice surfaces. However, given that the deviations were not consistent between each season and model, that both models exhibited large accumulated uncertainty, and that our interest was primarily at shorter timescales, we found no strong reasoning for tuning model parameters to fit model values precisely.

To ensure we could correctly simulate the large temporal variability in accumulation and ablation with each configuration of the model we also compared SMB over one-day

TCD

9, 975–1019, 2015

Cloud effects on the surface energy and mass balance of Brewster Glacier

J. P. Conway and
N. J. Cullen

Title Page

Abstract

Introduction

Conclusions

References

Tables

Figures

◀

▶

◀

▶

Back

Close

Full Screen / Esc

Printer-friendly Version

Interactive Discussion



Cloud effects on the surface energy and mass balance of Brewster Glacier

J. P. Conway and
N. J. Cullen

Title Page

Abstract

Introduction

Conclusions

References

Tables

Figures

◀

▶

◀

▶

Back

Close

Full Screen / Esc

Printer-friendly Version

Interactive Discussion



and 10 day periods (Fig. 4). SEBmr effectively captured the large variability in SMB during both accumulation and ablation seasons with maximum 10 day ablation and accumulation rates on the order of $50 \text{ mm w.e. day}^{-1}$ (Fig. 4b). A consistent bias in ablation was not observed, confirming our decision not to tune modelled melt exactly over the season. The significant number of large daily ablation events ($> 50 \text{ mm w.e. day}^{-1}$) observed in the ablation record were, in general, captured by SEBmr (Fig. 4a). If anything, a bias toward under-prediction of these events was seen. This bias is likely related to an under-prediction of QR, as the time-averaging P_{scaled} underestimated the very intense rainfall rates ($> 100 \text{ mm day}^{-1}$) associated with the largest ablation events (Gillett and Cullen, 2011). 10 day accumulation rates were captured well while daily totals exhibited much larger scatter, reflecting the difficulty of determining observed winter SMB from surface height records as well as the large combined uncertainty due to P_{scaled} , T_a and $T_{r/s}$. The good agreement of modelled and observed SMB at these short temporal resolutions suggests SEBmr is able to capture the variations in melt and accumulation forced by the key synoptic atmospheric controls.

SEBpr showed similar agreement to observed SMB at both daily and 10 day level (Fig. 4c and d). The larger uncertainty in modelled ablation was expected given the uncertainties involved in parameterising incoming radiation fluxes and albedo. A positive bias in modelled ablation rates was exhibited, though the 1 : 1 line is still well within the model uncertainty (2σ). This bias was likely an artefact of the limited value of the cloud extinction co-efficient (k), which produced a positive bias in ensemble mean $\text{SW}\downarrow$ as compared to the reference run (not shown). However, this bias was of less concern as the remaining analysis used the reference run and not the ensemble mean from the Monte Carlo runs to explore cloud effects on SMB and ΔSMB . That the temporal variability of SMB was effectively captured by SEBpr gives us confidence that this configuration captures the same atmospheric controls on SMB as SEBmr and as such provides a reliable and useful tool for sensitivity analysis.

3.2 Variation of SBL climate with cloudiness

The seasonal variation of surface climate in both clear-sky and overcast conditions during the measurement period is shown in Fig. 5a and b. Air temperature (T_a) exhibited a clear but relatively small ($\sim 8^\circ\text{C}$) seasonal cycle and was only slightly lower in overcast conditions compared to clear-sky conditions (Table 5). Vapour pressure (e_a) was significantly higher in overcast conditions, due to the similar T_a but markedly higher RH. Consequently in overcast conditions, mean e_a was above the saturated vapour pressure of a melting snow/ice surface (6.11 hPa) during December through April, while in clear-sky conditions mean e_a only reached this condition during February. Average T_s exhibited pronounced differences, being significantly higher in overcast conditions during every month. Average wind speed (U) was somewhat higher (0.1 to 0.7 m s^{-1}) in overcast conditions during most of the ablation season, while only small or non-significant differences with cloudiness were noted in other seasons (Table 3). Thus, the main changes in surface climate observed during cloudy periods were an increase in e_a , which, despite slightly lower T_a , were associated with a large increase in T_s .

3.3 Variation of SEB and melt with cloudiness

Monthly average SEB terms diagnosed using SEBmr showed marked variation with cloudiness and season during the measurement period (Fig. 5c and d). Clear-sky conditions were characterised by large and opposing fluxes. SWnet dominated the seasonal cycle, provided the largest source of energy during the summer months and peaked after the summer solstice in response to decreased albedo associated with the transition from a snow to ice surface in early January. LWnet remained a large sink throughout the year, creating strongly negative Rnet during the winter months (JJA) that drove cooling of the glacier surface. Low T_s in clear-sky conditions allowed QS to remain directed towards the surface throughout the year. QS was of a similar magnitude to LWnet and peaked during the winter months in response to an increase in both U and the surface–air temperature gradient (Fig. 5a and b). QL was much smaller in

Cloud effects on the surface energy and mass balance of Brewster Glacier

J. P. Conway and
N. J. Cullen

[Title Page](#)[Abstract](#)[Introduction](#)[Conclusions](#)[References](#)[Tables](#)[Figures](#)[⏪](#)[⏩](#)[◀](#)[▶](#)[Back](#)[Close](#)[Full Screen / Esc](#)[Printer-friendly Version](#)[Interactive Discussion](#)

magnitude than QS and of a generally negative sign, indicating that during clear-skies, sublimation or evaporation dominated over deposition or condensation. QR was absent and positive QC indicated that nocturnal cooling of the surface and subsurface was occurring. QM in excess of 20 W m^{-2} (equivalent to $5 \text{ mm w.e. day}^{-1}$) was present for a 7 month period between October and April (inclusive). In general the seasonal cycle of QM followed that of SWnet, but was modulated by variations in QL and QS.

In contrast to clear-skies, energy terms in overcast conditions were smaller in magnitude and directed towards the surface on average (Fig. 5d). SWnet was still the largest source of energy to the surface. LWnet was positive through most of the year, due to the enhancement of $\text{LW}\downarrow$ by low cloud cover and the T_s being limited to 0°C . Consequently, Rnet was positive throughout the year and larger than in clear-sky conditions from March to November (inclusive). QS and QL were nearly equal and both directed towards the surface, together producing a similar source of energy as Rnet. A distinct seasonal cycle in QS and QL was driven by the strong seasonal variation in surface–air temperature and moisture gradients in overcast conditions (Fig. 5b). QR made a small contribution to QM during the summer and QC was negligible. The net result was that despite the moderate magnitude of individual energy fluxes in overcast conditions, mean QM was similar to that in clear-sky conditions during most months and exceeded that in clear-sky conditions from February through May.

The similarity of mean QM in clear-sky and overcast conditions was due to a large extent to the fraction of time the surface was melting in each condition (Fig. 6). In clear-sky conditions, melt occurred for a much smaller fraction of time, reaching a maximum of 58 % during December, while in overcast conditions, melt occurred between 70 and 95 % of the time over the 7 months from October through April (inclusive). Day length during this period varied between 11.5 and 15.5 h, implying that nocturnal melt in overcast conditions was a significant feature during these months. While clear-sky and overcast conditions were experienced 36 and 45 % of the measurement period (Conway et al., 2014), they accounted for 30 and 50 % of total melt, respectively, as overcast conditions accounted for a much higher proportion of all melting periods.

Cloud effects on the surface energy and mass balance of Brewster Glacier

J. P. Conway and
N. J. Cullen

Title Page

Abstract

Introduction

Conclusions

References

Tables

Figures

◀

▶

◀

▶

Back

Close

Full Screen / Esc

Printer-friendly Version

Interactive Discussion



Cloud effects on the surface energy and mass balance of Brewster Glacier

J. P. Conway and
N. J. Cullen

Title Page

Abstract

Introduction

Conclusions

References

Tables

Figures

◀

▶

◀

▶

Back

Close

Full Screen / Esc

Printer-friendly Version

Interactive Discussion



When all melt periods were considered together (42 % of measurement period), SWnet made the largest contribution to QM, with QS and QL together contributing a little over one third and QR providing a non-negligible fraction (Table 6). On average LWnet and QC were energy sinks during melting periods, though as noted earlier they diverged strongly with cloudiness. Considering the average SEB terms in all periods, a shift towards QS at the expense of Rnet was observed, due to the inclusion of non-melting clear-sky periods, where negative LWnet was largely balanced by QS.

3.4 Sensitivity of SMB to changes in surface climate

Model runs with SEBpr over the sensitivity period (see Sect. 2.4) revealed a large Δ SMB to T_a (Table 7). The response to a ± 1 K change in T_a was much larger than that of a 20 % change in P_{scaled} and this large sensitivity is explored further in the following section. Increased RH induced a small mass loss, due to increased LW \downarrow and QL. Similarly, a mass loss of $0.79 \text{ m.w.e. a}^{-1}$ occurred for a 1 ms^{-1} increase in U , due to an increased contribution of turbulent heat fluxes to melt. The Δ SMB to terms controlling SWnet is surprisingly high, though no study has assessed this in the Southern Alps to date. A change in α of ± 0.1 induced over half the SMB response of $T_a \pm 1$ K (Table 7), while a 6 % decrease in SW_{TOA} (the approximate change in the solar constant during the last 10 000 years) only resulted in a modest change in SMB. Variations in the cloud extinction coefficient (k), within the uncertainty range of the radiation scheme optimisation (Conway et al., 2014), induced large mass changes, emphasising the fact that SWnet still makes the largest contribution to melt during overcast conditions (Table 6).

To examine how the large Δ SMB to T_a was expressed, a breakdown of SMB terms was constructed for the +1 and -1 K perturbation runs (Table 8). A change in snowfall accounted for 21 % of Δ SMB, while a small change in refreezing (2 %) and a dominant change in melt accounted for the remainder (77 %). Changes in deposition and sublimation were negligible. The large change in accumulation with T_a emphasises the temperate nature of the glacier SBL in the vicinity of $\text{AWS}_{\text{glacier}}$, where mean T_a dur-

Cloud effects on the surface energy and mass balance of Brewster Glacier

J. P. Conway and
N. J. Cullen

Title Page

Abstract

Introduction

Conclusions

References

Tables

Figures

◀

▶

◀

▶

Back

Close

Full Screen / Esc

Printer-friendly Version

Interactive Discussion

Clear-sky and partial cloud conditions showed more modest changes in melt, accounting for 29 and 21 % of the ΔSMB , respectively. By calculating the mean ΔSMB for clear-sky and overcast conditions in each month, a distinct seasonal cycle as well as a clear dependence on cloudiness emerged (Fig. 8). In general, the ΔSMB was greatly reduced during winter months, as T_a was well below $T_{r/s}$ at $\text{AWS}_{\text{glacier}}$ and ablation was minimal. On average, overcast conditions almost always produced higher ΔSMB than clear-skies, especially during spring and autumn. A peak in ΔSMB observed during October was associated with T_a around $T_{r/s}$ and a higher fraction of marginal melt conditions. ΔSMB in clear-sky conditions showed a long period of minimal ΔSMB from May through October (inclusive). January and February, however, show a large ΔSMB in clear-sky conditions, as the magnitude of SWnet was greatly influenced by the timing of the transition to an ice surface and summer snowfall. In order to isolate the snowdepth– α feedback, further runs of SEBpr were made for -1 and $+1$ K. By using measured α and perturbing $T_{r/s}$ with T_a , accumulation and SWnet remained consistent between these runs and the resulting ΔSMB (direct) was due to direct changes in QM only (Fig. 8., dashed lines). The divergence of full and direct ΔSMB in clear-skies conditions confirmed that changes in melt due to snowdepth– α feedbacks dominated clear-sky ΔSMB , especially in the summer. In overcast conditions, the direct ΔSMB is somewhat less than the full SMB, as periods with altered snowfall are removed. Still, the direct ΔSMB remained approximately twice as large as that in clear-sky conditions through each month. Thus, it is evident that cloudy conditions have a much stronger influence on ΔSMB to T_a than clear-sky conditions, with an increased ΔSMB in cloudy conditions being due to changes in both snowfall and melt, and being strongest in the spring and autumn seasons.

4 Discussion

4.1 Cloud impacts on SBL and SEB

The strong divergence of SEB with cloud condition seen in these results is driven in large part by changes in e_a , rather than changes in T_a . The increase in e_a in overcast conditions is enabled by the poor association of T_a and cloud cover, in addition to the obvious covariance between RH and cloudiness. That T_a is not markedly decreased in overcast conditions differs from similar studies in the European Alps (e.g. Pellicciotti et al., 2005) and Norway (Giesen et al., 2008), and is indicative of the maritime setting where air mass properties, rather than a positive association between summertime insolation and air temperature (Sicart et al., 2008), are the primary control on SBL variations (Cullen and Conway, 2015). The availability of moist and relatively warm air masses to the glacier surface also creates positive LWnet in overcast conditions, which along with increases in QL, allows for steady melt through much greater periods of time. Consequently, average daily melt rates are similar in clear-sky and overcast conditions, again in contrast with studies in the European Alps that show increased melt in clear-sky conditions (Pellicciotti et al., 2005). Glaciers in Norway (Giesen et al., 2008) show higher total melt during overcast conditions due to higher U that increase turbulent heat fluxes during frequent cloud cover. While increased U and turbulent heat fluxes are observed for the largest melt events on Brewster Glacier (Gillett and Cullen, 2011), mean U was not well differentiated by cloudiness over the measurement period, leaving T_a and e_a as the primary controls of mean QS and QL, respectively.

While LWnet was substantially increased during overcast periods, a “radiation paradox” (Ambach, 1974) does not occur during most of the melt season at Brewster Glacier, due to high SW_{TOA} , large cloud extinction coefficients and a smaller difference in sky emissivity in clear-sky and overcast conditions in this mid-latitude environment. In contrast, maritime sites on the melting margin of the Greenland ice sheet show clouds act to increase Rnet throughout the melt season at a range of elevations (van den Broeke et al., 2008a). At the lowest site where the surface is melting over 80 % of

Cloud effects on the surface energy and mass balance of Brewster Glacier

J. P. Conway and
N. J. Cullen

[Title Page](#)[Abstract](#)[Introduction](#)[Conclusions](#)[References](#)[Tables](#)[Figures](#)[◀](#)[▶](#)[◀](#)[▶](#)[Back](#)[Close](#)[Full Screen / Esc](#)[Printer-friendly Version](#)[Interactive Discussion](#)

Cloud effects on the surface energy and mass balance of Brewster Glacier

J. P. Conway and
N. J. Cullen

Title Page

Abstract

Introduction

Conclusions

References

Tables

Figures

◀

▶

◀

▶

Back

Close

Full Screen / Esc

Printer-friendly Version

Interactive Discussion



the summer period, the presence of a strong “radiation paradox” implies that melt rates are higher during overcast conditions, which is supported by the absence of increased summer melt during more frequent clear-sky conditions (van den Broeke et al., 2011). The lack of a “radiation paradox” during the summer months at Brewster Glacier emphasises the role of air mass properties that are advected from the surrounding ocean areas in maintaining T_a and enabling enhanced LWnet and QL during overcast periods. In the same way, during the transition periods, especially in the autumn, increased melt rates were enabled by a “radiation paradox”.

4.2 Cloud impacts on SMB sensitivity

The increased sensitivity of SMB to T_a in overcast conditions may help explain some of the high sensitivity of SMB in the Southern Alps. Importantly, average melt is not reduced in overcast conditions and cloud cover is frequent in the Southern Alps. Therefore, a large fraction of melt occurs in overcast conditions which are more sensitive to changes in T_a . In conjunction with increased e_a , clouds extend melt into periods of marginal melt that are more sensitive to changes in T_a as well as being strongly associated with frequent precipitation around $T_{r/s}$. Indeed, roughly half of the T_a sensitivity is due to accumulation–albedo feedbacks, in line with previous work in the Southern Alps (Oerlemans, 1997), emphasising the turbulent heat fluxes play a secondary role, despite the assertions of recent paleo-climatic research (Putnam et al., 2012). In addition, the largest melt events – which constitute a large fraction of melt over a season (Gillett and Cullen, 2011) – are associated with overcast conditions and contribute to proportionally larger changes in melt. Thus, air mass variability, in particular air temperature associated with high water vapour content, appears to be the primary control on melt during the summer ablation season.

Aside from their role in the Δ SMB to T_a , the contribution of turbulent heat fluxes to melt appears to have been overstated in a number of studies, at the expense of Rnet. In fact, the contribution of Rnet to ablation in the present study is similar to that found over mixed snow/ice ablation surfaces in Norway (68%; Giesen et al., 2008)

Cloud effects on the surface energy and mass balance of Brewster Glacier

J. P. Conway and
N. J. Cullen

Title Page

Abstract

Introduction

Conclusions

References

Tables

Figures

◀

▶

◀

▶

Back

Close

Full Screen / Esc

Printer-friendly Version

Interactive Discussion

Secondly, it follows that a change in the frequency of cloud cover or synoptic regime may enhance/dampen the SMB response to T_a . For example, a decrease in ΔSMB from west to east across the Southern Alps is likely, in association with the strong gradient of precipitation and cloudiness (Uddstrom et al., 2001). It is enticing to reduce the relationship between glacier mass balance and climate to the main causal mechanisms (i.e. temperature/precipitation paradigm). However, there is also the possibility that changes in atmospheric circulation coincident with changes in state variables in the past (i.e. during the last glacial maximum; Drost et al., 2007; Ackerley et al., 2011) may alter empirical relationships (i.e. TIM's) informed during the present climate, altering the climate signals derived from glacier fluctuations. For the Southern Alps, the most compelling analysis of the controls on SMB points to changes in the regional circulation patterns (Fitzharris et al., 2007), which are in turn associated with strong changes in both airmass properties and cloudiness (Hay and Fitzharris, 1988). Thus, it is likely that average relationships between melt and air temperature may indeed be changed if a shift to drier or wetter conditions is experienced.

The high fraction of melt due to SWnet and large contribution of snowfall–albedo feedbacks to ΔSMB also implies that local or regional influences on albedo may have an important role in modifying melt rate as seen in other areas (Oerlemans et al., 2009). Indeed the LGM period shows higher rates of glacial loess deposition in New Zealand (Eden and Hammond, 2003), thus the role of terrigenous dust in modifying glacier ablation rates during the onset of glacier retreat (e.g. Peltier and Marshall, 1995) is a topic that should be explored further in the context of the Southern Alps.

5 Conclusions

We have presented here a validated timeseries of SEB/SMB for a glacier surface in the Southern Alps of New Zealand during 2 annual cycles. High quality radiation data allowed a careful evaluation of the magnitude of SEB terms, as well as the selection of clear-sky and overcast conditions. An analysis of SBL climate and SEB showed a fun-

Cloud effects on the surface energy and mass balance of Brewster Glacier

J. P. Conway and
N. J. Cullen

Title Page

Abstract

Introduction

Conclusions

References

Tables

Figures

◀

▶

◀

▶

Back

Close

Full Screen / Esc

Printer-friendly Version

Interactive Discussion

damental change in SEB with cloudiness that was driven by an increase in effective sky emissivity and vapour pressure at the glacier surface. The only slightly diminished T_a during overcast periods created positive LWnet and also allowed both QS and QL to remain large and directed toward the surface. This created a strong increase in the fraction of time the surface was melting in overcast conditions, which led to a similar average melt rate in clear-sky and overcast conditions. Given the frequent cloud cover at the site, cloudy periods accounted for a majority of the melt observed, especially during autumn when SWnet inputs were lower.

A parameterisation of radiation components allowed the sensitivity of SMB to independent changes in SBL climate and shortwave radiation components to be assessed. The large sensitivity of SMB to T_a was expressed primarily through changes in snowfall and the associated positive α feedback. The remainder of this sensitivity was due to changes in the fraction of time the surface was melting and changes in the magnitude of QS, QL, LWnet and QR, in that order. The sensitivity of SMB to T_a diverged strongly when partitioned into clear-sky and overcast periods, with enhanced sensitivity during overcast periods due to both their covariance with precipitation and their ability to produce melt over large fractions of time. Increased sensitivity during overcast periods may explain some of the high sensitivity of SMB in the Southern Alps, and raises the possibility that the response of SMB to T_a in the past or future may be altered by changing synoptic patterns that are strongly associated with cloud cover. Thus, it highlights the need to include the effect of atmospheric moisture (vapour, cloud and precipitation) on both melt and accumulation processes when modelling glacier–climate interactions.

Acknowledgements. Funding from a University of Otago Research Grant (ORG10-10793101RAT) supported N. Cullen's contribution to this research. The research also benefited from the financial support of the National Institute of Water and Atmospheric Research, New Zealand (Climate Present and Past CLC01202), and collaboration with A. Mackintosh and B. Anderson, Victoria University of Wellington. The Department of Conservation supported this research under concession OT-32299-OTH. We thank T. Mølg for providing model code and for many helpful discussions on model development, as well as P. Sirguy and W. Colgan for help-

ful discussions on the Monte Carlo approach. D. Howarth and N. McDonald provided careful technical support for the field measurements.

References

- Ackerley, D., Lorrey, A., Renwick, J. A., Phipps, S. J., Wagner, S., Dean, S., Singarayer, J., Valdes, P., Abe-Ouchi, A., Ohgaito, R., and Jones, J. M.: Using synoptic type analysis to understand New Zealand climate during the Mid-Holocene, *Clim. Past*, 7, 1189–1207, doi:10.5194/cp-7-1189-2011, 2011.
- Ambach, W.: The influence of cloudiness on the net radiation balance of a snow surface with high albedo, *J. Glaciol.*, 13, 73–84, 1974.
- Anderson, B., Lawson, W., Owens, I., and Goodsell, B.: Past and future mass balance of “Ka Roimata o Hine Hukatere” Franz Josef Glacier, New Zealand, *J. Glaciol.*, 52, 597–607, doi:10.3189/172756506781828449, 2006.
- Anderson, B., Mackintosh, A., Stumm, D., George, L., Kerr, T., Winter-Billington, A., and Fitzsimons, S.: Climate sensitivity of a high-precipitation glacier in New Zealand, *J. Glaciol.*, 56, 114–128, doi:10.3189/002214310791190929, 2010.
- Blonquist, J. M., Tanner, B. D., and Bugbee, B.: Evaluation of measurement accuracy and comparison of two new and three traditional net radiometers, *Agr. Forest Meteorol.*, 149, 1709–1721, doi:10.1016/j.agrformet.2009.05.015, 2009.
- Chinn, T., Fitzharris, B. B., Willsman, A., and Salinger, M. J.: Annual ice volume changes 1976–2008 for the New Zealand Southern Alps, *Global Planet. Change*, 92, 105–118, doi:10.1016/j.gloplacha.2012.04.002, 2012.
- Conway, J. P.: Constraining Cloud and Airmass Controls on the Surface Energy and Mass Balance of Brewster Glacier, Southern Alps of New Zealand (PhD thesis), University of Otago, available at: <http://hdl.handle.net/10523/4432> (last access: 1 December 2014), 2013.
- Conway, J. P. and Cullen, N. J.: Constraining turbulent heat flux parameterization over a temperate maritime glacier in New Zealand, *Ann. Glaciol.*, 54, 41–51, doi:10.3189/2013AoG63A604, 2013.
- Conway, J. P., Cullen, N. J., Spronken-Smith, R. A., and Fitzsimons, S. J.: All-sky radiation over a glacier surface in the Southern Alps of New Zealand: characterizing cloud effects on

TCD

9, 975–1019, 2015

Cloud effects on the surface energy and mass balance of Brewster Glacier

J. P. Conway and
N. J. Cullen

Title Page

Abstract

Introduction

Conclusions

References

Tables

Figures

◀

▶

◀

▶

Back

Close

Full Screen / Esc

Printer-friendly Version

Interactive Discussion



Cloud effects on the surface energy and mass balance of Brewster GlacierJ. P. Conway and
N. J. Cullen

Title Page

Abstract

Introduction

Conclusions

References

Tables

Figures

◀

▶

◀

▶

Back

Close

Full Screen / Esc

Printer-friendly Version

Interactive Discussion



- Oerlemans, J.: Extracting a climate signal from 169 glacier records, *Science*, 308, 675–677, doi:10.1126/science.1107046, 2005.
- Oerlemans, J.: *The Microclimate of Valley Glaciers*, Igitur, Utrecht University, Utrecht, 2010.
- Oerlemans, J. and Knap, W. H.: A 1 year record of global radiation and albedo in the ablation-zone of Morteratschgletscher, Switzerland, *J. Glaciol.*, 44, 231–238, 1998.
- Oerlemans, J., Giesen, R. H., and Van den Broeke, M. R.: Retreating alpine glaciers: increased melt rates due to accumulation of dust (Vadret da Morteratsch, Switzerland), *J. Glaciol.*, 55, 729–736, doi:10.3189/002214309789470969, 2009.
- Pellicciotti, F., Brock, B., Strasser, U., Burlando, P., Funk, M., and Corripio, J.: An enhanced temperature-index glacier melt model including the shortwave radiation balance: development and testing for Haut Glacier d’Arolla, Switzerland, *J. Glaciol.*, 51, 573–587, doi:10.3189/172756505781829124, 2005.
- Peltier, W. R. and Marshall, S.: Coupled energy balance/ice-sheet model simulations of the glacial cycle: a possible connection between terminus and terrigenous dust, *J. Geophys. Res.*, 100, 14269–14289, 1995.
- Putnam, A. E., Schaefer, J. M., Denton, G. H., Barrell, D. J. A., Finkel, R. C., Andersen, B. G., Schwartz, R., Chinn, T. J. H., and Doughty, A. M.: Regional climate control of glaciers in New Zealand and Europe during the pre-industrial Holocene, *Nat. Geosci.*, 5, 627–630, doi:10.1038/ngeo1548, 2012.
- Sicart, J. E., Hock, R., and Six, D.: Glacier melt, air temperature, and energy balance in different climates: the Bolivian Tropics, the French Alps, and northern Sweden, *J. Geophys. Res.*, 113, D24113, doi:10.1029/2008JD010406, 2008.
- Sicart, J. E., Hock, R., Ribstein, P., and Chazarin, J. P.: Sky longwave radiation on tropical Andean glaciers: parameterization and sensitivity to atmospheric variables, *J. Glaciol.*, 56, 854–860, 2010.
- Tait, A. B. and Fitzharris, B. B.: Relationships between New Zealand rainfall and south-west Pacific pressure patterns, *Int. J. Climatol.*, 18, 407–424, doi:10.1002/(SICI)1097-0088(19980330)18:4<407:AID-JOC256>3.0.CO;2-S, 1998.
- Uddstrom, M. J., McGregor, J. A., Gray, W. R., and Kidson, J. W.: A high-resolution analysis of cloud amount and type over complex topography, *J. Appl. Meteorol.*, 40, 16–33, 2001.
- Ummenhofer, C. C. and England, M. H.: Interannual extremes in New Zealand precipitation linked to modes of Southern Hemisphere climate variability, *J. Climate*, 20, 5418–5440, doi:10.1175/2007JCLI1430.1, 2007.

Cloud effects on the surface energy and mass balance of Brewster Glacier

J. P. Conway and
N. J. Cullen

Title Page

Abstract

Introduction

Conclusions

References

Tables

Figures

◀

▶

◀

▶

Back

Close

Full Screen / Esc

Printer-friendly Version

Interactive Discussion



- van den Broeke, M. R., Van As, D., Reijmer, C., and Van de Wal, R.: Assessing and improving the quality of unattended radiation observations in Antarctica, *J. Atmos. Ocean. Tech.*, 21, 1417–1431, doi:10.1175/1520-0426(2004)021<1417:AAITQO>2.0.CO;2, 2004.
- van den Broeke, M., Reijmer, C., Van As, D., and Boot, W.: Daily cycle of the surface energy balance in Antarctica and the influence of clouds, *Int. J. Climatol.*, 26, 1587–1605, doi:10.1002/joc.1323, 2006.
- van den Broeke, M. R., Smeets, C. J. P. P., Ettema, J., and Kuipers Munneke, P.: Surface radiation balance in the ablation zone of the west Greenland ice sheet, *J. Geophys. Res.*, 113, D13105, doi:10.1029/2007JD009283, 2008a.
- van den Broeke, M., Smeets, P., Ettema, J., van der Veen, C., van de Wal, R., and Oerlemans, J.: Partitioning of melt energy and meltwater fluxes in the ablation zone of the west Greenland ice sheet, *The Cryosphere*, 2, 179–189, doi:10.5194/tc-2-179-2008, 2008b.
- van den Broeke, M. R., Smeets, C. J. P. P., and van de Wal, R. S. W.: The seasonal cycle and interannual variability of surface energy balance and melt in the ablation zone of the west Greenland ice sheet, *The Cryosphere*, 5, 377–390, doi:10.5194/tc-5-377-2011, 2011.
- Willis, I., Lawson, W., Owens, I., Jacobel, B., and Autridge, J.: Subglacial drainage system structure and morphology of Brewster Glacier, New Zealand, *Hydrol. Process.*, 23, 384–396, doi:10.1002/hyp.7146, 2009.

Cloud effects on the surface energy and mass balance of Brewster Glacier

J. P. Conway and
N. J. Cullen

Table 1. Variables measured, sensor specifications and mean annual values at AWS_{glacier}.

Variable	Instrument	Accuracy	Mean annual value
Air temperature (T_a)	Vaisala HMP 45AC	0.3 °C	1.2 °C
Relative humidity (RH)	Vaisala HMP 45AC	3 %	78 %
Wind speed (U)	RM Young 05103	0.3 ms ⁻¹	3.3 ms ⁻¹
Atmospheric pressure (p)	Vaisala PTB110	0.5 hPa	819 hPa
Incoming shortwave radiation ($SW\downarrow_{meas}$)	Kipp and Zonen CNR4	5 % ^a	140 W m ⁻²
Outgoing shortwave radiation ($SW\uparrow$)	Kipp and Zonen CNR4	5 % ^a	93 W m ⁻²
Incoming longwave radiation ($LW\downarrow_{meas}$)	Kipp and Zonen CNR4	5 % ^a	278 W m ⁻²
Surface temperature (T_s)	Kipp and Zonen CNR4	1 °C ^b	-2.7 °C
Precipitation (P_{scaled}) ^c	TB4 + Scaled ^c	25 % ^c	6125 mm ^c
Surface and sensor height	SR50a	±1 cm	n/a

^a Uncertainty is estimated to be less than the manufacturer's specifications as noted in van den Broeke et al. (2004) and Blonquist et al. (2009).

^b Based on a 5 W m⁻² uncertainty in $LW\uparrow$.

^c From AWS_{lake} during snow free period only. P_{scaled} is based on scaled relationship between AWS_{lake} and lowland station (Cullen and Conway, 2015). Uncertainty is estimated from fit of scaled relationship.

Title Page

Abstract

Introduction

Conclusions

References

Tables

Figures

◀

▶

◀

▶

Back

Close

Full Screen / Esc

Printer-friendly Version

Interactive Discussion



Cloud effects on the surface energy and mass balance of Brewster Glacier

J. P. Conway and
N. J. Cullen

Title Page

Abstract

Introduction

Conclusions

References

Tables

Figures

◀

▶

◀

▶

Back

Close

Full Screen / Esc

Printer-friendly Version

Interactive Discussion

Table 2. Configuration of SEBmr and SEBpr, showing input data and references used in the calculation of radiation terms in each configuration.

Variable	Model version	Reference and/or input data
α	SEBmr	Accumulated albedo (van den Broeke et al., 2004)
	SEBpr	Oerlemans and Knap (1998) (P_{scaled}, T_a)
SW↓	SEBmr	SW↓ _{surface}
	SEBpr	Conway et al. (2014) ($N_{\epsilon}, T_a, \text{RH}$)
LW↓	SEBmr	LW↓ _{meas}
	SEBpr	Conway et al. (2014) ($N_{\epsilon}, T_a, \text{RH}$)

Cloud effects on the surface energy and mass balance of Brewster Glacier

J. P. Conway and
N. J. Cullen

Title Page

Abstract

Introduction

Conclusions

References

Tables

Figures

◀

▶

◀

▶

Back

Close

Full Screen / Esc

Printer-friendly Version

Interactive Discussion



Table 3. Input parameter uncertainty introduced in Monte Carlo simulations of SMB uncertainty.

Input parameter	Value(s)	Systematic [random] error	Model
Roughness length for momentum (z_{0v}) ^a	3.6×10^{-3} m	$z_{0v} \times 10^{\text{NORMRND}(0,0.274)}$	SEBmr, pr
Rain/snow threshold ($T_{r/s}$) ^b	1.0 °C	0.3 [0.5]	SEBmr, pr
Albedo of surface ($\alpha_{\text{snow}}, \alpha_{\text{firn}}, \alpha_{\text{ice}}$) ^b	0.95 (α_{snow}) 0.65 (α_{firn}) 0.42 (α_{ice})	0.05	SEBpr
Constant for cloud extinction coefficient ^c	0.1715	0.0048 [0.0048]	SEBpr
Multiplier for cloud extinction coefficient ^c	0.07182 hPa ⁻¹	0.0324 [0.0324]	SEBpr
Albedo of surrounding terrain ^d	0.45	0.1	SEBpr
Clear-sky emissivity constant ^e	0.456 Pa ⁻¹ K	0.0204 [0.0204]	SEBpr

^a SD of z_{0v} (Conway and Cullen, 2013). NORMRND is a MATLAB function that selects a random number from a normal distribution with mean of 0 and SD of 0.274.

^b Macguth et al. (2008).

^c 95 % confidence interval of optimised coefficients (Conway et al., 2014). Limited to 0.95.

^d Assumed; no random errors as terrain albedo will not vary at this timescale (30 min).

^e RMSD of clear-sky values (Conway et al., 2014).

Cloud effects on the surface energy and mass balance of Brewster Glacier

J. P. Conway and
N. J. Cullen

Title Page

Abstract

Introduction

Conclusions

References

Tables

Figures

⏪

⏩

◀

▶

Back

Close

Full Screen / Esc

Printer-friendly Version

Interactive Discussion



Table 4. Observed and modelled SMB (m.w.e.) for selected periods between stake measurements in ablation (Abl) and accumulation (Acc) seasons. Figure 2b shows the length of each period.

Period	Observed	SEBmr	SEBpr
Abl 1 snow	−1.74	−1.78	−1.67
Abl 1 ice	−3.35	−2.92	−3.28
Acc1	1.52	1.40	1.46
Abl 2 snow	−1.51	−1.78	−1.48
Abl 2 ice	−1.94	−1.87	−1.66

Cloud effects on the surface energy and mass balance of Brewster Glacier

J. P. Conway and
N. J. Cullen

Table 5. Mean differences in surface climate between clear-sky and overcast conditions. Positive values indicate an increase in overcast conditions.

Variable	Jan	Feb	Mar	Apr	May	Jun	Jul	Aug	Sep	Oct	Nov	Dec	Annual
T_a (°C)	-1.3	-0.2	-0.8	-3	-0.9	-0.5	-1.3	-1.2	-0.7	-0.1	-1.4	-1.2	-1.1
RH (%)	35	25	35	53	44	39	52	37	45	33	34	37	39
e_a (hPa)	2.5	2.2	2.5	3.1	2.6	2.2	2.6	1.7	2.3	2.1	2	2.7	2.4
U (ms ⁻¹)	0.6	0.1	0.6	-0.2	-0.1	0	0	-0.2	-0.1	-0.1	0.2	0.7	0.1
T_s (°C)	0.5	0.3	0.9	1.5	4.7	5.4	6.3	5.2	5.8	2.6	1.5	0.6	2.9
ρ (hPa)	-7	-4	-8	-6	-10	-7	-12	-4	-9	-3	-7	-8	-7

Bold face indicates monthly differences are significant at the 95 % level using a two sided t test assuming unequal variances. Temperature and wind speed are normalised to 2 m values.

[Title Page](#)
[Abstract](#)
[Introduction](#)
[Conclusions](#)
[References](#)
[Tables](#)
[Figures](#)
[Back](#)
[Close](#)
[Full Screen / Esc](#)
[Printer-friendly Version](#)
[Interactive Discussion](#)

Cloud effects on the surface energy and mass balance of Brewster Glacier

J. P. Conway and
N. J. Cullen

Table 6. Average surface energy fluxes ($W m^{-2}$) for melting periods in clear-sky and overcast conditions, all melting periods, and all periods during the measurement period. Bracketed bolds show the proportion of QM for each condition.

	SWnet	LWnet	Rnet	QS	QL	QR	QC	QM
Melting + clear-sky periods	240 (121)	-67 (-34)	173 (87)	39 (20)	-7 (-3)	0 (0)	-6 (-3)	199
Melting + overcast periods	36 (33)	15 (14)	51 (46)	30 (27)	24 (22)	7 (7)	-2 (-2)	110
Melting periods	96 (70)	-8 (-6)	88 (65)	32 (24)	15 (11)	5 (3)	-3 (-2)	136
All periods	49 (83)	-27 (-46)	22 (37)	31 (53)	2 (3)	2 (4)	2 (3)	58

Melting conditions are selected as periods where $QM > 0$ in SEBmr.

[Title Page](#)
[Abstract](#)
[Introduction](#)
[Conclusions](#)
[References](#)
[Tables](#)
[Figures](#)
[◀](#)
[▶](#)
[◀](#)
[▶](#)
[Back](#)
[Close](#)
[Full Screen / Esc](#)
[Printer-friendly Version](#)
[Interactive Discussion](#)


Cloud effects on the surface energy and mass balance of Brewster Glacier

J. P. Conway and
N. J. Cullen

Title Page

Abstract

Introduction

Conclusions

References

Tables

Figures

◀

▶

◀

▶

Back

Close

Full Screen / Esc

Printer-friendly Version

Interactive Discussion

Table 7. Δ SMB (mm w.e. a^{-1}) to changes in surface climate and shortwave radiation terms. Values are averages of positive and negative perturbation runs of SEBpr over the sensitivity period, while the sign of Δ SMB is shown for an increased in each input variable or parameter.

Variable and perturbation	Δ SMB
$T_a \pm 1 \text{ K}$	-2065
$P_{\text{scaled}} \pm 20 \%$	+770
$\text{RH} \pm 10 \%$	-380
$U \pm 1 \text{ m s}^{-1}$	-790
$\alpha \pm 0.1$	+1220
Solar constant -6 %	-260
$k \pm 0.17$	-740

Cloud effects on the surface energy and mass balance of Brewster Glacier

J. P. Conway and
N. J. Cullen

Title Page

Abstract

Introduction

Conclusions

References

Tables

Figures

◀

▶

◀

▶

Back

Close

Full Screen / Esc

Printer-friendly Version

Interactive Discussion

Table 8. Sum of SMB terms for selected runs of SEBpr over the two year sensitivity period. All units are in mm w.e., except for Δ which is in mm w.e. $K^{-1} a^{-1}$.

Scenario	SMB	Snowfall	Melt	Sublimation	Deposition	Refreezing
+1 K	−9181	3900	13 064	32	134	85
−1 K	−920	5670	6692	38	135	198
Δ (mm w.e. $K^{-1} a^{-1}$)	−2065	443	−1593	2	0	28

Cloud effects on the surface energy and mass balance of Brewster Glacier

J. P. Conway and
N. J. Cullen

Table 9. Mean SEB terms during melting periods in the +1 K (A) and –1 K (B) perturbation runs of SEBpr. Also shown are mean SEB terms in the –1 K perturbation run, for the same periods as A, i.e. melting periods in the +1 K perturbation run (C), and the increases between each scenario (D, E). The contribution of each flux to QM, or the increase in QM, is given in bracketed bolds.

Scenario	SWnet	LWnet	Rnet	QS	QL	QR	QC	QM
A: +1 K melting periods	89 (62)	–4 (–3)	85 (59)	37 (26)	19 (14)	5 (3)	–2 (–1)	144
B: –1 K melting periods	70 (68)	–9 (–8)	61 (60)	28 (27)	11 (11)	4 (4)	–2 (–2)	103
C: –1 K for same periods as A	56 (76)	–13 (–17)	43 (59)	23 (32)	7 (9)	3 (4)	–2 (–2)	74
D: increase from B to A	19 (46)	5 (11)	23 (57)	9 (22)	8 (20)	1 (2)	0 (0)	41
E: increase from C to A	33 (47)	8 (12)	41 (59)	14 (20)	13 (18)	2 (3)	0 (0)	70

[Title Page](#)
[Abstract](#)
[Introduction](#)
[Conclusions](#)
[References](#)
[Tables](#)
[Figures](#)
[◀](#)
[▶](#)
[◀](#)
[▶](#)
[Back](#)
[Close](#)
[Full Screen / Esc](#)
[Printer-friendly Version](#)
[Interactive Discussion](#)

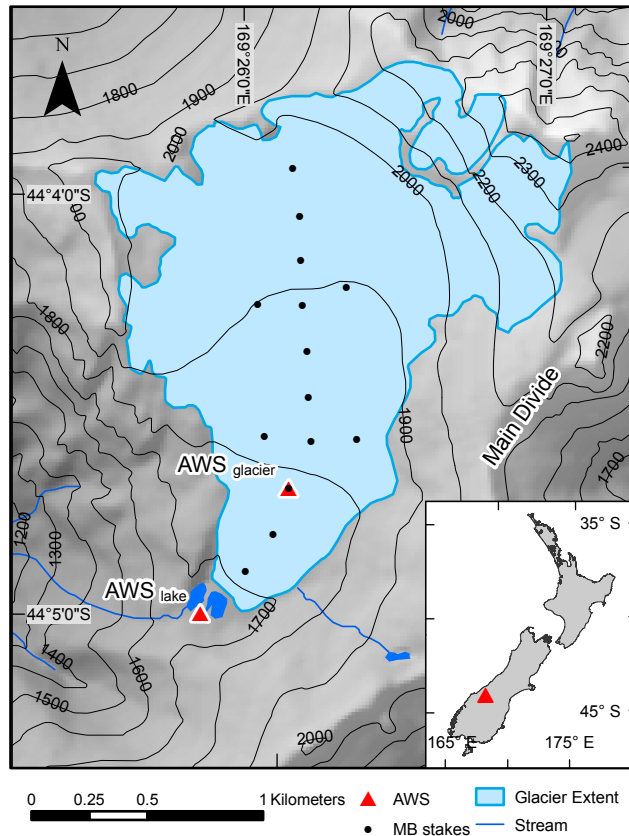



Figure 1. Map of Brewster Glacier showing AWS locations and surrounding topography. Contour lines are at 100 m intervals. Long-term mass balance network (MB stakes) shown as filled circles. The glacier margin shown is based on a 1997 GPS survey (Willis et al., 2009). The ridgeline to the southeast of the glacier is the main divide of the Southern Alps. The inset map shows the location of Brewster Glacier within New Zealand.

Cloud effects on the surface energy and mass balance of Brewster Glacier

J. P. Conway and N. J. Cullen

Title Page

Abstract Introduction

Conclusions References

Tables Figures

◀ ▶

◀ ▶

Back Close

Full Screen / Esc

Printer-friendly Version

Interactive Discussion



Cloud effects on the surface energy and mass balance of Brewster Glacier

J. P. Conway and
N. J. Cullen

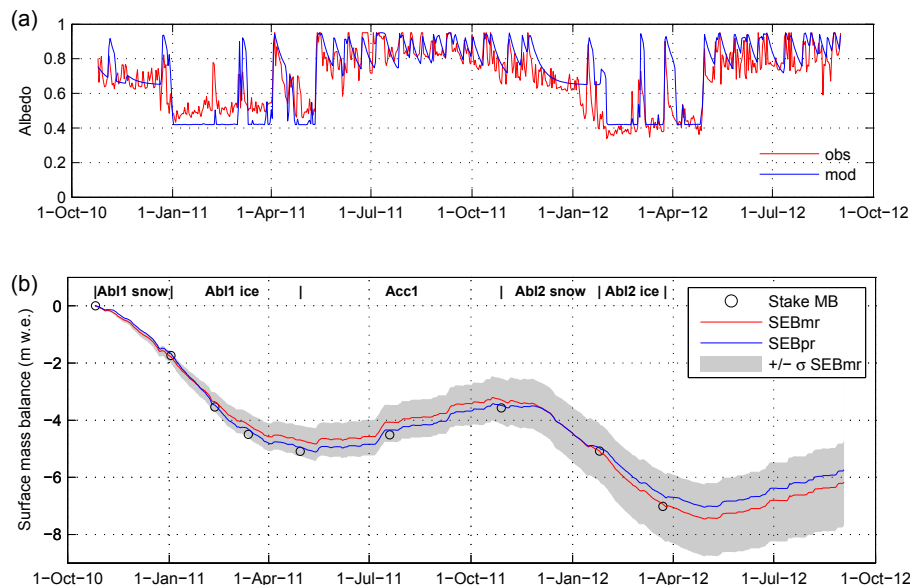


Figure 2. (a) Daily average albedo observed at $AWS_{glacier}$ (red) during the measurement period and modelled in SEBpr (blue) using the expressions of Oerlemans and Knap (1998), with optimised coefficients. (b) Accumulated SMB during the measurement period as modelled by the reference runs of SEBmr and SEBpr. The points give observed mass balance from periodic stake and snow pit measurements. The SMB for selected ablation and accumulation periods (shown as Abl1 snow etc.) are given in Table 4. The shaded envelope shows ± 1 SD from the mean of SEBmr, calculated using Monte Carlo simulations (see Sect. 2.4 for details).

[Title Page](#)
[Abstract](#)
[Introduction](#)
[Conclusions](#)
[References](#)
[Tables](#)
[Figures](#)
[Back](#)
[Close](#)
[Full Screen / Esc](#)
[Printer-friendly Version](#)
[Interactive Discussion](#)

Cloud effects on the surface energy and mass balance of Brewster Glacier

J. P. Conway and
N. J. Cullen

Title Page

Abstract

Introduction

Conclusions

References

Tables

Figures

◀

▶

◀

▶

Back

Close

Full Screen / Esc

Printer-friendly Version

Interactive Discussion

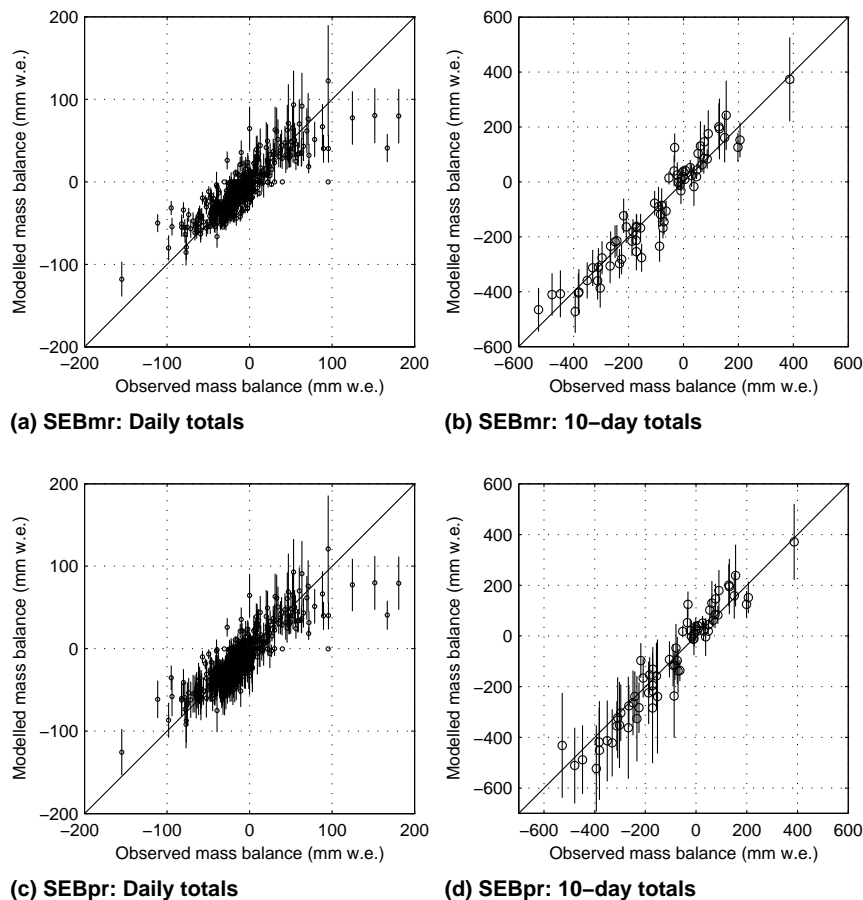


Figure 4. Observed vs. modelled mass balance for **(a, b)** SEBmr and **(c, d)** SEBpr over 1 day and 10 day periods. Error bars show $\pm 2\sigma$ from the ensemble mean values.

Cloud effects on the surface energy and mass balance of Brewster Glacier

J. P. Conway and
N. J. Cullen

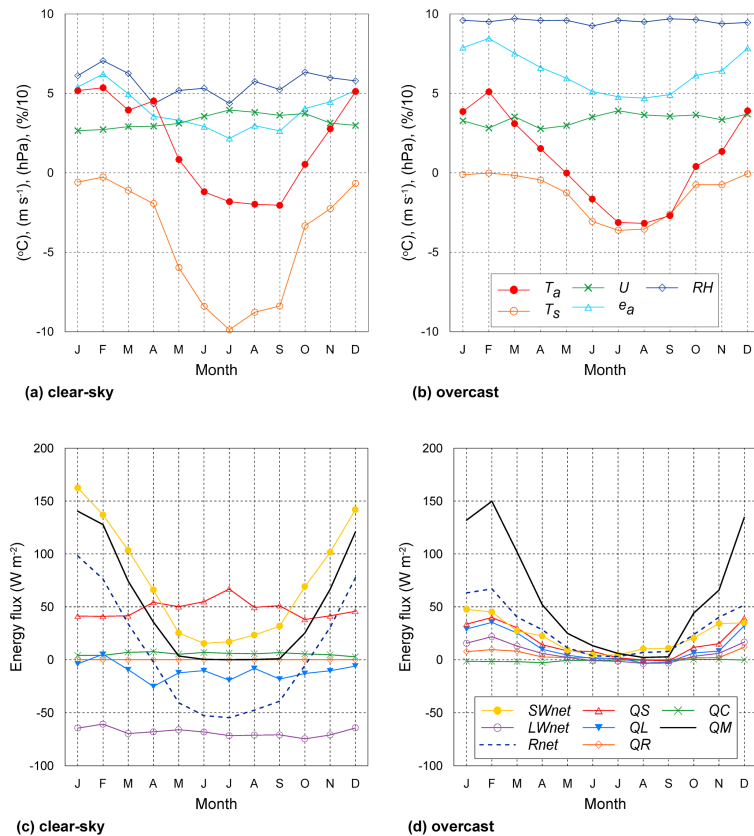


Figure 5. Monthly mean surface climate (**a**, **b**) and surface energy fluxes (**c**, **d**) at $AWS_{glacier}$ in (**a**, **c**) clear-sky and (**b**, **d**) overcast conditions. Partial cloud conditions are a graduation between the two extremes and are not shown for brevity. Surface climate variables include air and surface temperature ($^{\circ}C$), wind speed ($m s^{-1}$), vapour pressure (hPa), and relative humidity on a scale from 0 to 10 (i.e. %/10).

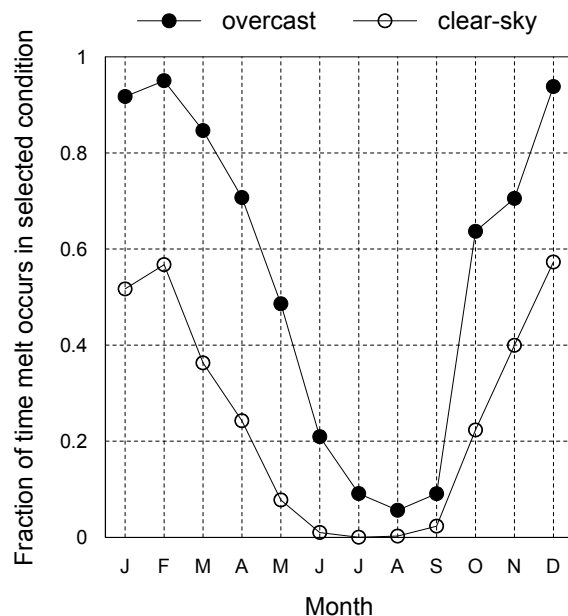
Cloud effects on the surface energy and mass balance of Brewster GlacierJ. P. Conway and
N. J. Cullen

Figure 6. Fraction of time surface melting occurred in clear-sky (open circles) and overcast (closed circles) conditions during each month. Melting conditions are selected as periods where $QM > 0$ in SEBmr.

[Title Page](#)[Abstract](#)[Introduction](#)[Conclusions](#)[References](#)[Tables](#)[Figures](#)[◀](#)[▶](#)[◀](#)[▶](#)[Back](#)[Close](#)[Full Screen / Esc](#)[Printer-friendly Version](#)[Interactive Discussion](#)

Cloud effects on the surface energy and mass balance of Brewster Glacier

J. P. Conway and
N. J. Cullen

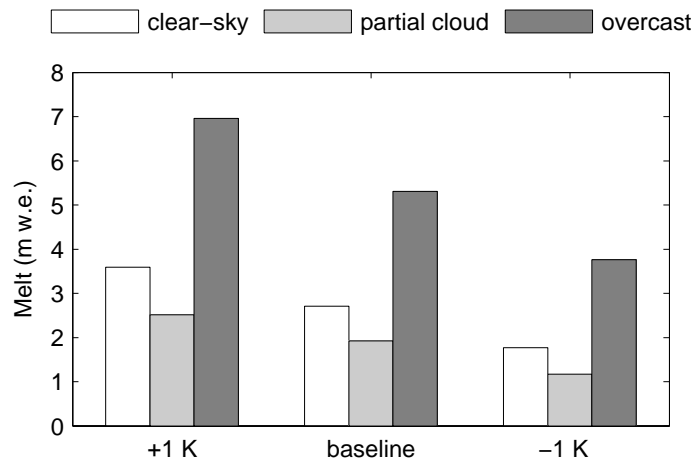


Figure 7. Total surface melt in each cloud cover category for reference and climate perturbation scenarios.

[Title Page](#)[Abstract](#)[Introduction](#)[Conclusions](#)[References](#)[Tables](#)[Figures](#)[◀](#)[▶](#)[◀](#)[▶](#)[Back](#)[Close](#)[Full Screen / Esc](#)[Printer-friendly Version](#)[Interactive Discussion](#)

Cloud effects on the surface energy and mass balance of Brewster Glacier

J. P. Conway and
N. J. Cullen

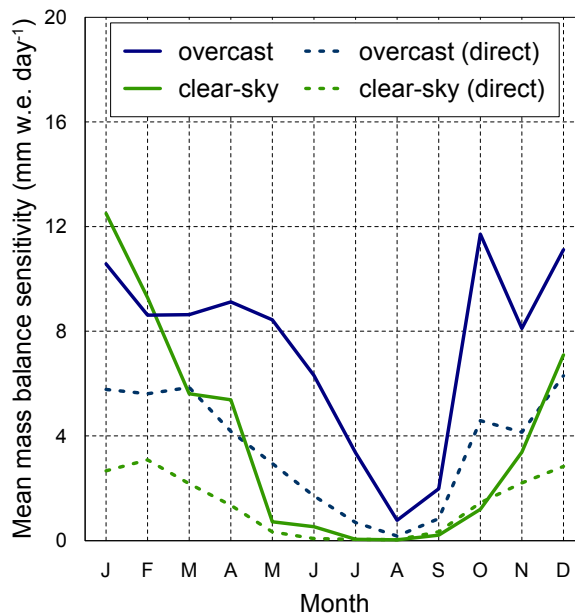


Figure 8. The mean daily mass balance sensitivity (ΔSMB) to a 1 K change in T_a , separated into clear-sky (green) and overcast (blue) conditions, in each month of the year. The dashed lines show ΔSMB resulting from only a direct change in QM, which was derived from a further model run using measured albedo and perturbing $T_{r/s}$ with T_a . The positive values indicate mass loss for increased T_a .

[Title Page](#)
[Abstract](#)
[Introduction](#)
[Conclusions](#)
[References](#)
[Tables](#)
[Figures](#)
[◀](#)
[▶](#)
[◀](#)
[▶](#)
[Back](#)
[Close](#)
[Full Screen / Esc](#)
[Printer-friendly Version](#)
[Interactive Discussion](#)